

# Spin waves and stability of zigzag order in the Hubbard model with spin-dependent hopping terms - Application to the honeycomb lattice compounds $\text{Na}_2\text{IrO}_3$ and $\alpha - \text{RuCl}_3$

Shubhajyoti Mohapatra and Avinash Singh\*

*Department of Physics, Indian Institute of Technology, Kanpur - 208016, India*

(Dated: December 14, 2024)

Spin waves in the zigzag ordered antiferromagnetic state on a honeycomb lattice are investigated within a Hubbard model with spin-dependent hopping terms. Roles of the emergent Kitaev, Heisenberg, Dzyaloshinskii-Moriya, and symmetric-off-diagonal spin interactions are investigated on the stability of the zigzag order. While the DM interactions are found to strongly destabilize the zigzag order, the secondary spin-dependent hopping terms (associated with structural distortions) are shown to strongly stabilize the zigzag order and account for magnetocrystalline anisotropy, easy axis, and spin wave gap. The calculated spin wave dispersion and energy scale are in good agreement with inelastic neutron scattering measurements on  $\alpha - \text{RuCl}_3$  and  $\text{Na}_2\text{IrO}_3$ .

## I. INTRODUCTION

Involving strong spin-orbit coupling (SOC), transition metal oxides of the  $5d$  group are of considerable recent interest in view of potential technological importance and novel electronic and magnetic properties such as topological band or Mott insulators, quantum spin liquids, field-induced topological order, topological superconductors, and spin-orbital Mott insulators. The compounds  $A_2\text{IrO}_3$  ( $A = \text{Li, Na}$ ), in which edge-sharing  $\text{IrO}_6$  octahedra form a honeycomb lattice, have been predicted to display novel magnetic states for composite spin-orbital moments including Néel, zigzag, and stripy antiferromagnetic (AFM) order.<sup>1</sup>

Dispersive spin-wave excitations have been measured in inelastic neutron scattering (INS) and resonant inelastic X-ray scattering (RIXS) experiments providing overall energy scale of spin excitations and the relevant magnetic interactions, showing that substantial further-neighbor exchange couplings are required to explain the observed dispersion. For  $\text{Na}_2\text{IrO}_3$ , spin wave excitations have been identified below 6 meV in INS studies,<sup>1</sup> although found extending up to 35 meV in RIXS studies, with additional peaks in the range  $0.4 < \omega < 0.8$  eV associated with the excitonic modes.<sup>2</sup> For  $\alpha - \text{RuCl}_3$ , INS measurements show spin wave gap of  $\sim 2$  meV around the  $M'$  point of the Brillouin zone.<sup>3</sup>

Extended range spin couplings have been ascribed, in the case of  $\text{Na}_2\text{IrO}_3$ , to sizable  $t_{sp\sigma}$  hopping parameter involving the higher Na  $s$  orbitals. Single-crystal diffraction and local-density approximation calculations have been combined to revise the crystal structure for the spin-orbit coupled honeycomb antiferromagnet  $\text{Na}_2\text{IrO}_3$ , highlighting important departures from the ideal case where the Kitaev exchange dominates.<sup>1</sup>

With strong SOC and rather weak Coulomb correlation of  $5d$  electrons known as key ingredients in determining the ground state properties of the  $5d$  transition metal oxides  $\text{Sr}_2\text{IrO}_4$  and  $\text{Na}_2\text{IrO}_3$ , whether they should be classified as Mott or Slater type insulators has attracted considerable attention recently.<sup>4-8</sup> In the Slater picture, with the quasi-molecular orbital as appropriate basis for incorporating the strong anisotropic hybridization between  $5d$  orbitals of neighboring Ir atoms, the zigzag AFM ordering is seen as due to energy gain from the gap opening at the zone boundary.<sup>9</sup> On the other hand, in the Mott picture the appropriate basis to describe the local electronic structure is obtained from the on-site atomic SOC and the crystal field, and the superexchange formalism used to describe the zigzag-type AFM ordering accounts for the observed PM insulating state well above  $T_N$ .<sup>4,5,10</sup>

However, the detailed nature of the magnetic interactions and energy excitations required raise questions on the validity of the superexchange-based formalism.<sup>11</sup>

Although multi-peak features in photoemission spectrum and optical conductivity seem to support the Slater picture, it is hard to explain the observed PM insulating state well above  $T_N$ , and the central issue appears to be whether local AFM ordering is essential in describing the insulating state of  $\text{Na}_2\text{IrO}_3$  or not.<sup>8</sup> Using density functional theory and dynamical mean field theory, the temperature-dependent electronic structure of  $\text{Na}_2\text{IrO}_3$  has been investigated recently. While the calculated photoemission spectrum in the paramagnetic state shows that the insulating state persists even above the Néel temperature, indicating a Mott character, analysis of the optical conductivity indicates that non-local correlation effect of Ir  $5d$  electrons are important as well in describing its electronic and magnetic properties, suggesting that  $\text{Na}_2\text{IrO}_3$  is not a standard Mott insulator.<sup>8</sup>

The honeycomb family of iridium oxides ( $\text{A}_2\text{IrO}_3$ ,  $\text{A}=\text{Na},\text{Li}$ ) and  $\alpha - \text{RuCl}_3$  are unique in that they constitute an approximate realization of the Heisenberg-Kitaev (HK) model,<sup>12</sup> with the Kitaev term emerging as the dominant interaction.<sup>5,13-17</sup> Extensive studies of the HK model focussing on the anisotropic part of the magnetic interactions in these compounds also predict some nontrivial properties like spin liquid state and phase transitions involving different magnetic ground states. However, within the HK model with nearest-neighbor interactions, it is difficult to account for both the zigzag magnetic order<sup>11</sup> as well as the magnetic excitation spectrum in  $\text{Na}_2\text{IrO}_3$  measured by RIXS and neutron scattering experiments.<sup>1,18,19</sup> Additional exchange paths and symmetric-off-diagonal interactions have therefore been included in models for the honeycomb lattice iridates and ruthenates.<sup>1,5,20-23</sup>

In contrast to the  $J_{\text{eff}} = 1/2$  localized spin HK model (strong SOC), formation of quasi-molecular orbitals (QMO) has been suggested with weak role of SOC,<sup>9</sup> and DFT calculations show that  $\text{Na}_2\text{IrO}_3$  is close to an itinerant regime, with delocalization of electron over individual Ir hexagons. The delocalised nature of electrons is also indicated from X-ray absorption spectroscopy (XAS), suggesting finite orbital mixing between  $J=1/2$  and  $3/2$  states in  $\text{Na}_2\text{IrO}_3$ .<sup>6</sup> An extensive investigation of electronic properties of  $\text{Na}_2\text{IrO}_3$  in the framework of DFT calculations shows behavior in-between the fully itinerant and the fully localized descriptions.<sup>11</sup>

Iridates and  $\alpha - \text{RuCl}_3$ , the only two known material systems that were proposed as candidates for the Kitaev spin liquid, instead show long range zigzag magnetic order. Sev-

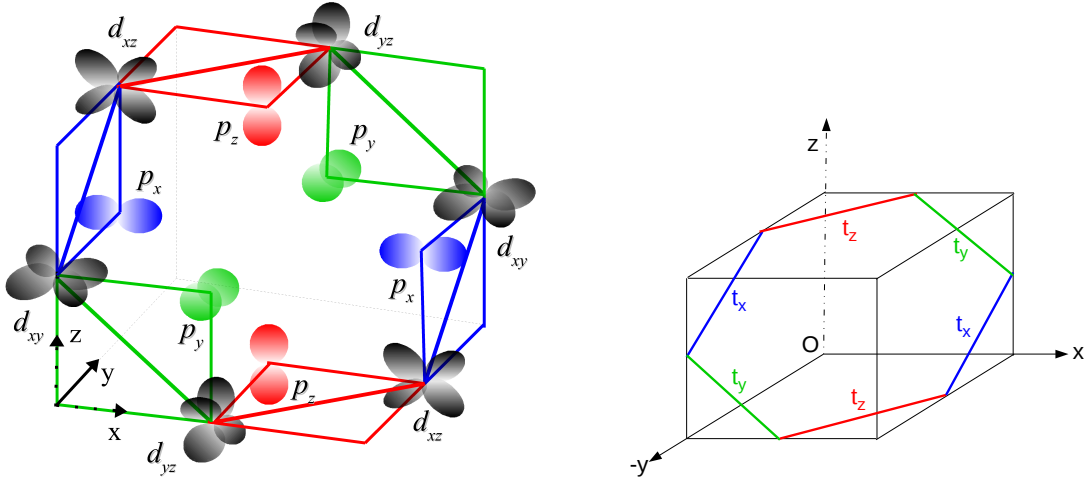


FIG. 1: Schematic representation of the honeycomb lattice structure of Ir in the cubic setting. For each of the three types of Ir-Ir bonds, O-assisted hopping between only two particular  $t_{2g}$  orbitals is possible:  $d_{yz} - d_{xz}$  (red),  $d_{xz} - d_{xy}$  (blue), and  $d_{xy} - d_{yz}$  (green). Two possible hopping paths via oxygen  $p$  orbitals are shown. Similar Cl-assisted hopping leads to orbital mixing in  $\alpha - \text{RuCl}_3$ .

eral recent experimental studies have shown that magnetic order can be fully suppressed by an external magnetic field applied parallel to the honeycomb plane.<sup>24,25</sup> The strongly anisotropic magnetization and magnetic susceptibility in presence of applied magnetic field is ascribed to the strongly anisotropic g-factor.<sup>26</sup> Further theoretical studies of spin dynamics in the presence of a magnetic field and field-induced quantum spin liquid state should be particularly intriguing.

In this paper, we will investigate spin dynamics in the zigzag state within a Hubbard model on the honeycomb lattice with spin-dependent hopping terms arising from the orbital mixing between the  $t_{2g}$  orbitals due to the O-assisted hopping. This will allow for a microscopic and unified understanding of the roles of the emergent Kitaev, Heisenberg, Dzyaloshinskii-Moriya (DM), and symmetric-off-diagonal (SOD) interactions on the stabilization of zigzag order and measured spin wave excitations in the honeycomb lattice compounds. Spin wave dispersion in these compounds have been investigated in earlier theoretical works within the three-orbital Hubbard model,<sup>27</sup> but not within the Kitaev-Hubbard model.<sup>28</sup>

## II. ORBITAL MIXING AND SPIN-DEPENDENT HOPPING

Honeycomb lattice iridates contain edge-sharing  $\text{IrO}_6$  octahedra, and relative orientations of neighboring  $\text{IrO}_6$  octahedra give rise to different dominant hopping pathways between the  $t_{2g}$  orbitals located on Ir ions at the centre of these octahedra.<sup>29</sup> There are two Ir-O-Ir hopping paths with  $90^\circ$  bonding geometry between two neighboring Ir ions, and the O-assisted hopping ( $\pi$  overlap) between unlike Ir orbitals gives rise to effective orbital mixings. Specifically, dominant orbital mixing terms between  $d_{xz} - d_{yz}$ ,  $d_{yz} - d_{xy}$ ,  $d_{xy} - d_{xz}$  orbitals are induced by the O-assisted hopping for nearest-neighbor Ir sites in the same  $z$ ,  $y$ ,  $x$  planes, respectively (Figure 1).

Transforming from the three-orbital basis to the  $J_{\text{eff}}$  basis, where the  $3/2$  and  $1/2$  sectors are well separated in the strong SOC limit, the mixing terms between  $d_{xz} - d_{yz}$ ,  $d_{yz} - d_{xy}$ ,  $d_{xy} - d_{xz}$  orbitals result in spin-dependent hopping terms  $t_z, t_y, t_x$  in the  $J_{\text{eff}} = 1/2$  sector.<sup>30</sup> We therefore consider the one-band Hubbard model on the honeycomb lattice:

$$H = -t_1 \sum_{\langle ij \rangle} (a_{i\sigma}^\dagger a_{j\sigma} + H.c.) - t_2 \sum_{\langle ik \rangle} (a_{i\sigma}^\dagger a_{k\sigma} + H.c.) + \sum_{\langle ij \rangle, \mu} \psi_i^\dagger [-i\sigma_\mu t_\mu] \psi_j + U \sum_i a_{i\uparrow}^\dagger a_{i\uparrow} a_{i\downarrow}^\dagger a_{i\downarrow} \quad (1)$$

where  $t_1, t_2$  are the usual first and second neighbor hopping terms,  $t_\mu$  represent the spin-dependent hopping terms which are alternately  $t_x / t_y / t_z$  around each honeycomb plaquettes as shown in Fig. 2, and  $U$  is the local Coulomb interaction term. The spin-dependent hopping terms  $t_\mu$  are restricted to only first neighbors for simplicity. Here  $a_{i,\sigma}$  represents the electron annihilation operator and  $\psi_i = (a_{i\uparrow} a_{i\downarrow})$  for site  $i$ .

## III. ZIGZAG STATE ON THE HONEYCOMB LATTICE

We now consider the above Hamiltonian (1) in the Hartree-Fock (HF) approximation corresponding to magnetic ordering in the  $z$  direction. In a composite four-sublattice, two-spin basis corresponding to the zigzag magnetic order shown in Fig. 2(a), the HF Hamiltonian

matrix is obtained as:

$$H_{\text{HF}}^{\sigma}(\mathbf{k}) = \begin{bmatrix} \varepsilon_{k2}^{(b)} - \Delta & 0 & \varepsilon_{k1}^{(a)} & \varepsilon_{kx} + \varepsilon_{ky} & \varepsilon_{k1}^{(b)} + \varepsilon_{kz} & 0 & \varepsilon_{k2}^{(a)} & 0 \\ & \varepsilon_{k2}^{(b)} + \Delta & \varepsilon_{kx} - \varepsilon_{ky} & \varepsilon_{k1}^{(a)} & 0 & \varepsilon_{k1}^{(b)} - \varepsilon_{kz} & 0 & \varepsilon_{k2}^{(a)} \\ & & \varepsilon_{k2}^{(b)} - \Delta & 0 & \varepsilon_{k2}^{(a)} & 0 & \varepsilon_{k1}^{(b)*} + \varepsilon_{kz}^* & 0 \\ & & & \varepsilon_{k2}^{(b)} + \Delta & 0 & \varepsilon_{k2}^{(a)} & 0 & \varepsilon_{k1}^{(b)*} - \varepsilon_{kz}^* \\ & & & & \varepsilon_{k2}^{(b)} + \Delta & 0 & \varepsilon_{k1}^{(a)*} & \varepsilon_{kx}^* - \varepsilon_{ky}^* \\ & & & & & \varepsilon_{k2}^{(b)} - \Delta & \varepsilon_{kx}^* + \varepsilon_{ky}^* & \varepsilon_{k1}^{(a)*} \\ & & & & & & \varepsilon_{k2}^{(b)} + \Delta & 0 \\ & & & & & & & \varepsilon_{k2}^{(b)} - \Delta \end{bmatrix} \quad (2)$$

where the band terms corresponding to normal and spin-dependent hoppings in different directions are given by:

$$\begin{aligned} \varepsilon_{k1}^{(a)} &= -2t_1 e^{-ik_x/2} \cos(\sqrt{3}k_y/2) \\ \varepsilon_{k1}^{(b)} &= -t_1 e^{ik_x} \\ \varepsilon_{k2}^{(a)} &= -4t_2 \cos(3k_x/2) \cos(\sqrt{3}k_y/2) \\ \varepsilon_{k2}^{(b)} &= -2t_2 \cos(\sqrt{3}k_y) \\ \varepsilon_{kx} &= -it_x e^{-i(k_x/2 - \sqrt{3}k_y/2)} \\ \varepsilon_{ky} &= -t_y e^{-i(k_x/2 + \sqrt{3}k_y/2)} \\ \varepsilon_{kz} &= -it_z e^{ik_x} \end{aligned} \quad (3)$$

and  $\Delta = mU/2$  is the staggered field in terms of the sublattice magnetization:

$$m(\Delta) = (n_{\uparrow}^A - n_{\downarrow}^A)(\Delta) = (n_{\uparrow}^B - n_{\downarrow}^B)(\Delta) = (n_{\downarrow}^C - n_{\uparrow}^C)(\Delta) = (n_{\downarrow}^D - n_{\uparrow}^D)(\Delta) \quad (4)$$

which is determined self-consistently from the electronic densities calculated from  $H_{\text{HF}}^{\sigma}(\mathbf{k})$  for the two spins  $\sigma = \uparrow, \downarrow$  on the four magnetic sublattices. In practice, it is easier to choose  $\Delta$  and determine  $U$  from the calculated sublattice magnetization  $m(\Delta)$ . In the large  $U$  limit,  $2\Delta \approx U$  as  $m \rightarrow 1$ . We will consider only the half-filled case ( $n = 1$ ) with Fermi energy in the AFM band gap.

#### IV. SPIN WAVES IN THE ZIGZAG AFM STATE

In the following, we will consider transverse spin fluctuations in the  $x$  and  $y$  directions in the zigzag ordered state (Fig. 2) with magnetic ordering in the  $z$  direction. These low-energy collective excitations, studied earlier within the Kitaev-Heisenberg localized spin models,<sup>12</sup>

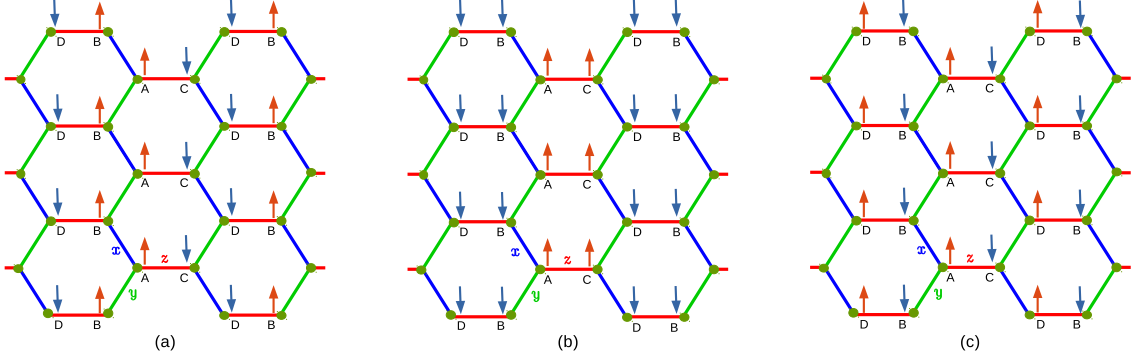


FIG. 2: The zigzag (a), stripy (b), and Néel (c) magnetic orders on the honeycomb lattice, showing the four sublattices (A,B,C,D). The spin-dependent hopping terms are alternately  $t_x / t_y / t_z$  around each honeycomb plaquette, as indicated by  $x, y, z$  with blue, green, and red bonds.

will include the gapless Goldstone mode corresponding to specific spin twisting modes which transform the ground state from one zigzag domain to another, and will also show the spin wave gap resulting from the intrinsic magnetic anisotropy due to the spin-dependent hopping terms (see Appendix).

Due to the spin mixing terms in Hamiltonian (1), spin is not a good quantum number, and we therefore use the method developed earlier for the  $120^\circ$  (non-collinear) ordering on the triangular lattice to investigate transverse spin fluctuations.<sup>31</sup> We consider the time-ordered transverse spin fluctuation propagator:

$$[\chi(\mathbf{q}, \omega)]_{\alpha\beta}^{\mu\nu} = i \int dt e^{i\omega(t-t')} \sum_j e^{-i\mathbf{q}\cdot(\mathbf{r}_i - \mathbf{r}_j)} \langle \Psi_G | T[S_i^\mu(t) S_j^\nu(t')] | \Psi_G \rangle \quad (5)$$

where  $\mu, \nu = x, y$  are the transverse spin directions and  $\alpha, \beta$  are the sublattice indices corresponding to sites  $i, j$ . In the random phase approximation (RPA),<sup>31</sup>

$$[\chi(\mathbf{q}, \omega)] = \frac{\frac{1}{2} [\chi^0(\mathbf{q}, \omega)]}{\mathbf{1} - U[\chi^0(\mathbf{q}, \omega)]} \quad (6)$$

where the bare particle-hole propagator  $[\chi^0(\mathbf{q}, \omega)]$  is obtained by integrating out the fermions in the broken-symmetry state. For the half-filled insulating state, the added hole (-) / particle (+) states lie in the lower / upper Hubbard band, and we have

$$[\chi^0(\mathbf{q}, \omega)]_{\alpha\beta}^{\mu\nu} = \frac{1}{2} \sum_{klm} \frac{\langle \sigma^\mu \rangle_\alpha^{-+} \langle \sigma^\nu \rangle_\beta^{-+*}}{E_{\mathbf{k}-\mathbf{q},m}^+ - E_{\mathbf{k},l}^- + \omega} + \frac{\langle \sigma^\mu \rangle_\alpha^{+-} \langle \sigma^\nu \rangle_\beta^{+-*}}{E_{\mathbf{k},l}^+ - E_{\mathbf{k}-\mathbf{q},m}^- - \omega}, \quad (7)$$

where  $E_{\mathbf{k},l}$  are the eigenvalues of the HF Hamiltonian matrix (2),  $l, m$  are the branch indices and  $\langle \sigma^\mu \rangle_\alpha$  denotes the spin matrix element for component  $\mu = x, y$  on the  $\alpha$  sublattice

between particle-hole states:

$$\langle \sigma^\mu \rangle_\alpha^{-+} \equiv \langle \mathbf{k} - \mathbf{q}, m, + | \sigma^\mu | \mathbf{k}, l, - \rangle_\alpha. \quad (8)$$

The bare particle-hole propagator  $[\chi^0(\mathbf{q}, \omega)]_{\alpha,\beta}^{\mu\nu}$  is a  $[8 \times 8]$  Hermitian matrix in the composite four-sublattice ( $\alpha=A,B,C,D$ ) and two spin-component ( $\mu = x, y$ ) basis. The (real) eigenvalues  $\lambda_{\mathbf{q}}(\omega)$  and eigenvectors  $|\phi_{\mathbf{q}}(\omega)\rangle$  contain information about the collective spin wave modes. Also included are the particle-hole (Stoner) excitations across the band gap, given by the poles of  $[\chi^0(\mathbf{q}, \omega)]_{\alpha,\beta}^{\mu\nu}$ . In the following, we will focus on the spin-wave energies  $\omega_{\mathbf{q}}$ , which are obtained from the poles  $1 - U\lambda_{\mathbf{q}}(\omega_{\mathbf{q}}) = 0$  of Eq. (6).

It is instructive to start with the strong-coupling expansion and consider the various spin interaction terms generated up to second order in the hopping terms (Appendix A). The DM term is absent for  $t = 0$ , resulting in the Kitaev-Heisenberg model, for which there are three equivalent zigzag domains, with specific spin twisting modes transforming from one domain to another (Appendix B).

The calculated spin-wave dispersion  $\omega_{\mathbf{q}}$  along different symmetry directions of the Brillouin zone are discussed below. Figs. 3 (a,c) show the zero-energy mode at the  $M'$  point (midway between  $\Gamma$  and  $K$ ) for the case  $t_1 = t_2 = 0$  (no DM interaction and no magnetic frustration). This Goldstone mode corresponds to the spin twisting mode discussed above, which costs zero energy even in the presence of magnetic anisotropy. The overall softening of the spin wave spectrum (lower branch) when  $t$  is turned on reflects the frustration effect due to the Heisenberg interaction  $(4t^2/U)\mathbf{S}_i \cdot \mathbf{S}_j$  (Figs. 3 (b,d). The strong instability at  $M'$  is exclusively due to the DM interactions (which require both  $t$  and  $t_\mu$  to be non-zero). This is consistent with the absence of this instability for  $t_1 = t_2 = 0$ . Furthermore, for  $t_2 = 0$ , we find that this instability develops *for any finite*  $t_1$ , which cannot be accounted in terms of the Kitaev and Heisenberg interactions only (Appendix B), thus confirming the significant role of the DM interactions on the stability of zigzag order. As DM interactions are intrinsically present in our Hubbard model analysis, a stronger destabilization of zigzag order is obtained than in earlier works on the KH model.

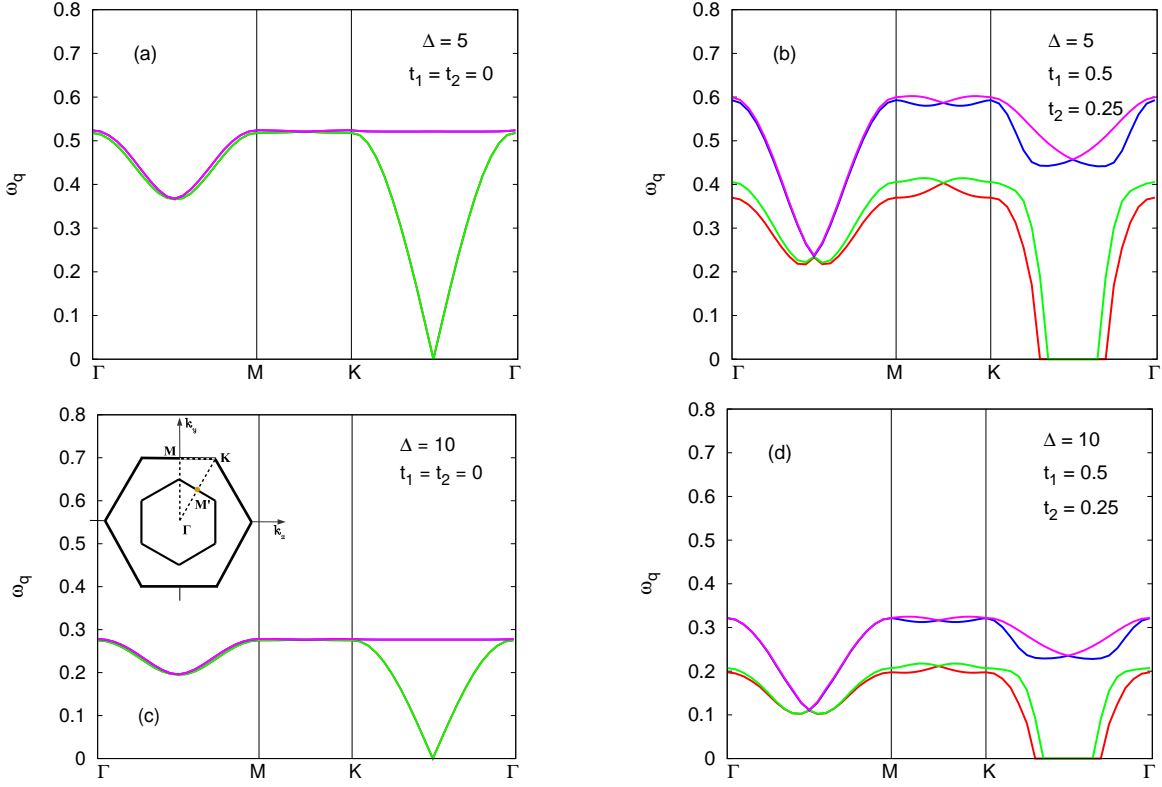


FIG. 3: Calculated spin wave energies in the zigzag ordered state with (a,c) only spin-dependent hopping terms  $t_\mu = 1$  ( $\mu = x, y, z$ ), and (b,d) including finite  $t_1 = 0.5$  and  $t_2 = 0.25$  for (a,b)  $\Delta = 5$  and (c,d)  $\Delta = 10$ . The spin wave energies approximately scale as  $t^2/U$ . Inset in (c) shows the extended and magnetic Brillouin zones.

### Stabilization of zigzag order

In order to suppress the instability near  $M'$  arising from the DM interaction-induced spin canting, we will now study the effects of reduced hopping parameters ( $t_n^{(p)} < t_n^{(ap)}$ ) for the frustrated (parallel) spins compared to the unfrustrated (antiparallel) spins, which results in net positive energy cost for the spin twisting mode (Appendix B). This reduced frustration results in significant stabilization of the zigzag order as seen in Fig. 4(a) for hopping parameter values  $t_1^{(p)} = 0.7t_1^{(ap)}$ ,  $t_2^{(p)} = 0.2$ , and  $t_2^{(ap)} = 0.3$ , showing only a marginal instability at  $M'$ , in contrast to the strong instability seen in Fig. 3(b).

Furthermore, this marginal instability in the strong coupling limit is removed at intermediate coupling, as seen in Fig. 4(b). This novel finite- $U$ -induced stabilization of zigzag order is due to the second neighbor ferromagnetic spin couplings  $J_2^{(p)}(U)$  induced at finite  $U$

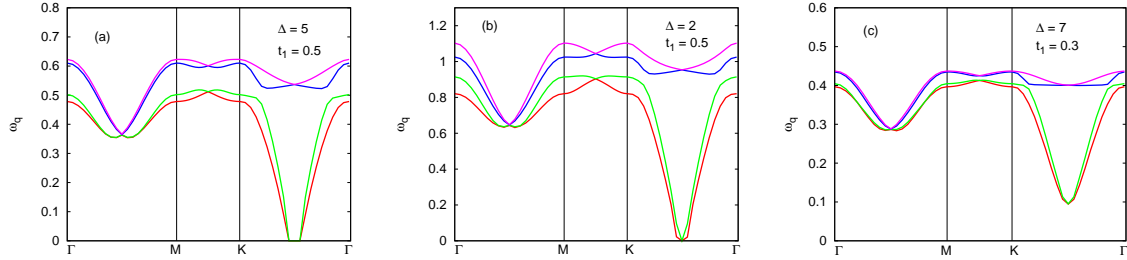


FIG. 4: Stabilization of the zigzag order near M' due to finite- $U$ -induced spin couplings (a,b) and emergence of finite gap with further suppression of the magnetic frustration (c).

between parallel spins. This interaction also results in positive energy cost for the spin twisting mode from one domain to another (Appendix B). Further suppression of the frustration results in finite spin wave gap at M' as shown in Fig. 4(c), where  $t_1 = 0.3$ ,  $t_1^{(p)} = 0.5t_1$ ,  $t_2^{(p)} = 0.15$ ,  $t_2^{(ap)} = 0.25$ , and  $\Delta = 7$ .

Finally, in order to investigate the magnetocrystalline anisotropy and easy axis, we will consider secondary spin-dependent hopping terms arising from structural distortions. We have therefore included small spin-dependent hopping terms  $\tilde{t}_x$  ( $\tilde{t}_y$ ) along the  $y$  ( $x$ ) bonds. Thus  $t_x \rightarrow (t_x, \tilde{t}_y)$  and  $t_y \rightarrow (\tilde{t}_x, t_y)$ . From the strong-coupling expansion (Appendix A), magnetocrystalline anisotropy and easy axis (along  $S_z$  direction) is readily seen, along with the onset of symmetric-off-diagonal spin interactions. Similarly, including secondary spin-dependent hopping terms along the  $y, z$  ( $z, x$ ) bonds will result in easy axis along the  $S_x$  ( $S_y$ ) direction in spin space. Figure 5 shows the spin wave dispersion for  $\tilde{t}_x = \tilde{t}_y = 0.2$ ,  $t_1 = 0.1$ ,  $t_2 = 0$  and  $\Delta = 10$  ( $U \approx 20$ ), with the energy scale  $t_\mu = 30$  meV. Features of the calculated spin wave dispersion are in qualitative agreement with the INS and RIXS measurements on  $\alpha$ -RuCl<sub>3</sub> and Na<sub>2</sub>IrO<sub>3</sub>.<sup>1-3</sup>

For this choice of parameters, the value of  $U \approx 0.6$  eV is similar to that obtained in spin wave studies of the one-band Hubbard model for Sr<sub>2</sub>IrO<sub>4</sub>.<sup>30</sup> Using the transformation from the three-orbital basis to the  $J_{\text{eff}}$  basis, the intra-orbital Coulomb interaction  $U_\mu = 3U$  is in agreement with estimates from DFT studies and experiments.

The honeycomb materials of interest adopt monoclinic  $C2/m$  structure, and the distortion results in metal-legand-metal bond angle different from 90°, which can be as large as 100° in Na<sub>2</sub>IrO<sub>3</sub>. The distortion-induced reduction in the local octahedral crystal field symmetry modifies the O-assisted hoppings which can introduce additional (secondary) orbital mixings.<sup>22,32</sup> In view of the substantial magneto-crystalline anisotropy, spin wave gap, and

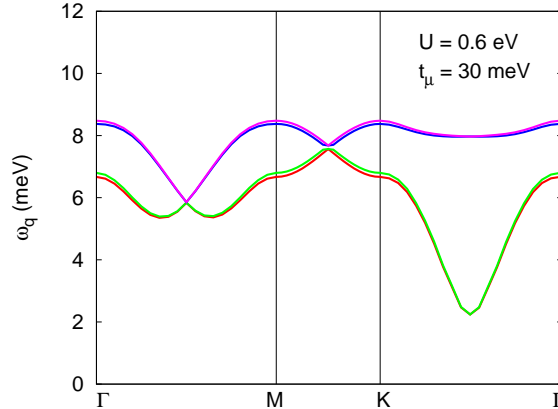


FIG. 5: Calculated spin wave energies with realistic energy scales for the hopping and interaction terms. Here  $t_1 = 0.1$ ,  $t_2 = 0$ ,  $\Delta = 10$  ( $U \approx 20$ ), and energy scale  $t_\mu = 30$  meV.

stabilization of zigzag order, the sensitive dependence on the secondary spin-dependent hopping terms arising from the structural distortions highlights an interesting interplay between magnetic order and crystal distortion.

In the parameter regime where zigzag order is stable (positive spin wave energies over the entire BZ), we find that the stripy and Néel orders show negative spin wave energies over substantial parts of the BZ. This confirms the relative stability of the zigzag order due to the anisotropic magnetic interactions generated by the spin-dependent hopping terms arising from orbital mixing.

The essential features of the calculated spin wave dispersion are summarized here: (i) Spin wave gap at  $\Gamma$  due to the anisotropic Kitaev interactions. (ii) Decreasing spin wave energy (sinusoidal) along the  $\Gamma$  - M direction ( $q_x = 0$ ,  $q_y = \text{finite}$ ) with minimum near the midpoint (phase angle  $\sqrt{3}q_y/2 = \pi/2$ ) reflecting the reduced energy cost due to  $\cos(\sqrt{3}q_y/2)$  factor in the  $S_z$  component on the B (D) sublattice. (iii) Goldstone mode at  $M'$  corresponding to the spin twisting from one zigzag domain to another (Fig. 6). (iv) Overall spin wave softening due to the  $J$ -induced frustration. (v) Destabilization of zigzag order near  $M'$  due to DM-induced spin canting. (vi) Novel finite- $U$ -induced stabilization of zigzag order. (vii) Strong stabilization of zigzag order by secondary spin-dependent hopping terms which are responsible for magnetocrystalline anisotropy, easy axis, and spin wave gap at  $M'$ . (viii) Positive spin wave energies over the entire Brillouin zone for zigzag order and negative energy modes over significant parts of the BZ for stripy and Néel orders.

## V. CONCLUSIONS

Spin waves in the zigzag-ordered antiferromagnetic state on a honeycomb lattice were investigated within a Hubbard model with spin-dependent hopping terms, focussing on the roles of the emergent Kitaev, Heisenberg, Dzyaloshinskii-Moriya, and symmetric-off-diagonal spin interactions on the stability of the zigzag order. While the anisotropic Kitaev interactions favor zigzag order, the DM interactions were found to strongly destabilize this order by inducing spin canting. Highlighting the importance of structural distortions, the secondary spin-dependent hopping terms introduced in the model were shown to strongly stabilize the zigzag order (consistent with similar finding on including symmetric-off-diagonal interactions in spin models) and also account for magnetocrystalline anisotropy, easy axis, and spin wave gap. The calculated spin wave features are in good agreement with inelastic neutron scattering measurements on  $\alpha$ -RuCl<sub>3</sub> and Na<sub>2</sub>IrO<sub>3</sub>.

Effects of the second neighbor spin-dependent hopping terms on spin dynamics, not included in the present work, should also be interesting in view of their significant magnitude as indicated from band structure studies. The strong magnetic frustration resulting from the  $t_{2z}$  terms between parallel spins will significantly reduce the spin wave energy scale, leading to closer agreement between the O-assisted orbital mixing hopping terms obtained from band structure studies and our spin-dependent hopping energy scale extracted by comparing the calculated spin wave dispersion with experiments.

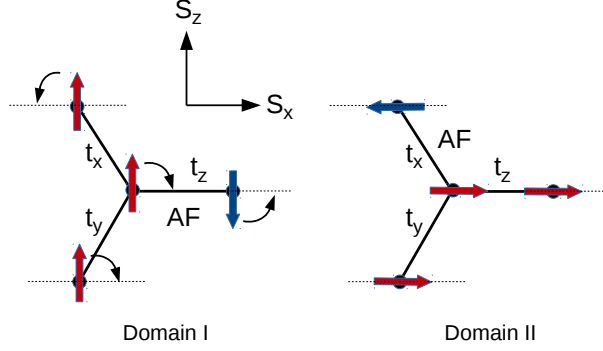


FIG. 6: Existence of  $120^\circ$ -twinned magnetic domains for the zigzag order, connected by specific spin twisting modes as shown, results in the gapless Goldstone mode even in the presence of anisotropic spin interactions.

### Appendix A: Strong-coupling expansion and anisotropic spin interactions

Starting with the Hubbard model (Eq. 1), the various anisotropic spin interactions (Kitaev, Dzyaloshinskii-Moriya, pseudo-dipolar, symmetric-off-diagonal) generated in the strong coupling expansion due to both the spin-dependent hopping terms  $t_\mu$  and the normal hopping terms  $t$  are obtained as:

$$\begin{aligned}
 H_{\text{eff}}^{(2)} = & \frac{4t_x^2}{U} \sum_{\langle ij \rangle} [S_i^x S_j^x - (S_i^y S_j^y + S_i^z S_j^z) - n_i n_j] \\
 & + \frac{4t_y^2}{U} \sum_{\langle ij \rangle} [S_i^y S_j^y - (S_i^z S_j^z + S_i^x S_j^x) - n_i n_j] \\
 & + \frac{4t_z^2}{U} \sum_{\langle ij \rangle} [S_i^z S_j^z - (S_i^x S_j^x + S_i^y S_j^y) - n_i n_j] \\
 & + \frac{8tt_z}{U} \sum_{\langle ij \rangle} (\mathbf{S}_i \times \mathbf{S}_j) \cdot \hat{z} + \frac{8tt_x}{U} \sum_{\langle ij \rangle} (\mathbf{S}_i \times \mathbf{S}_j) \cdot \hat{x} + \frac{8tt_y}{U} \sum_{\langle ij \rangle} (\mathbf{S}_i \times \mathbf{S}_j) \cdot \hat{y} \\
 & + \frac{8t_x t_y}{U} \sum_{\langle ij \rangle} (S_i^x S_j^y + S_i^y S_j^x) + \frac{8t_y t_z}{U} \sum_{\langle ij \rangle} (S_i^y S_j^z + S_i^z S_j^y) + \frac{8t_z t_x}{U} \sum_{\langle ij \rangle} (S_i^z S_j^x + S_i^x S_j^z) \\
 & + \frac{4t^2}{U} \sum_{\langle ij \rangle} [\mathbf{S}_i \cdot \mathbf{S}_j - n_i n_j]
 \end{aligned} \tag{A1}$$

Here we have considered a general case where all three hopping terms  $t_\mu$  are present for a given  $\langle ij \rangle$  pair. The symmetric-off-diagonal terms ( $S_i^\alpha S_j^\beta$ ) are generated only if two components  $t_\alpha$  and  $t_\beta$  of the spin-dependent hopping terms are non-zero for the same pair  $\langle ij \rangle$ , and have been included in recent studies to stabilize the zigzag order.<sup>5</sup>

## Appendix B: Zigzag domains and Goldstone mode

As seen from Fig. 6, the AFM aligned spins correspond to the pair of sites with spin-dependent hopping  $t_z$  ( $t_x$ ) for the zigzag domain I (II). The specific spin twisting mode (Fig. 6) allows for continuously transforming from one zigzag domain to another. The classical interaction energy is invariant under this continuous transformation as shown below, indicating the existence of a zero-energy Goldstone mode at the appropriate wave vector.

For spin twisting by angle  $\theta$  with respect to  $S_z$  axis in the  $S_z - S_x$  plane, the classical interaction energy for the pair of sites connected by hopping  $t_z$  is obtained from the corresponding spin interaction terms:

$$E(t_z) = \frac{4t_z^2}{U} [S_i^z S_j^z - (S_i^x S_j^x + S_i^y S_j^y)] = \frac{4t_z^2}{U} S^2 [-\cos^2 \theta - \sin^2 \theta] \quad (\text{B1})$$

which is independent of the twist angle  $\theta$ . The energy increase in the  $z$  term is exactly compensated by the energy decrease in the  $x$  term. Similar energy compensation results for the pair of sites connected by hopping terms  $t_x$  and  $t_y$ .

In contrast, for the isotropic exchange interactions  $J = (4t^2/U)\mathbf{S}_i \cdot \mathbf{S}_j$ , the energy invariance follows from an exact cancellation of the *different* contributions associated with a given site. If the exchange interactions between parallel and antiparallel spins are denoted by  $J_n^{(p)}$  and  $J_n^{(ap)}$  for first and second neighbors ( $n = 1, 2$ ), the net energy cost:

$$\Delta E = \left( J_1^{(ap)} - J_1^{(p)} \right) [1 - \cos 2\theta] + \left( J_2^{(ap)} - J_2^{(p)} \right) [1 - \cos 2\theta] \quad (\text{B2})$$

which identically vanishes in the frustrated case  $J_n^{(p)} = J_n^{(ap)}$ . However, for reduced frustration  $J_n^{(p)} < J_n^{(ap)}$  (or equivalently  $t_n^{(p)} < t_n^{(ap)}$  in terms of the hopping parameters), the net energy cost becomes positive.

## Acknowledgement

Helpful discussions with Jeroen van den Brink and Rajyavardhan Ray, and sponsorship grant from the Alexander von Humboldt Foundation for a research stay at IFW Dresden (AS) are gratefully acknowledged.

---

\* Electronic address: avinas@iitk.ac.in

- <sup>1</sup> S. K. Choi, R. Coldea, A. N. Kolmogorov, T. Lancaster, I. I. Mazin, S. J. Blundell, P. G. Radaelli, Y. Singh, P. Gegenwart, K. R. Choi, S.-W. Cheong, P. J. Baker, C. Stock, and J. Taylor, *Phys. Rev. Lett.* **108**, 127204 (2012).
- <sup>2</sup> H. Gretarsson, J. P. Clancy, Y. Singh, P. Gegenwart, J. P. Hill, J. Kim, M. H. Upton, A. H. Said, D. Casa, T. Gog, and Y.-J. Kim, *Phys. Rev. B* **87**, 220407(R) (2013).
- <sup>3</sup> K. Ran, J. Wang, W. Wang, Z.-Y. Dong, X. Ren, S. Bao, S. Li, Z. Ma, Y. Gan, Y. Zhang, J. T. Park, G. Deng, S. Danilkin, S.-L. Yu, J.-X. Li, and J. Wen, *Phys. Rev. Lett.* **118**, 107203 (2017).
- <sup>4</sup> R. Comin, G. Levy, B. Ludbrook, Z.-H. Zhu, C. N. Veenstra, J. A. Rosen, Y. Singh, P. Gegenwart, D. Stricker, J. N. Hancock, D. van der Marel, I. S. Elfimov, and A. Damascelli, *Phys. Rev. Lett.* **109**, 266406 (2012).
- <sup>5</sup> J. Chaloupka, G. Jackeli, and G. Khaliullin, *Phys. Rev. Lett.* **110**, 097204 (2013).
- <sup>6</sup> C. H. Sohn, H.-S. Kim, T. F. Qi, D. W. Jeong, H. J. Park, H. K. Yoo, H. H. Kim, J.-Y. Kim, T. D. Kang, D.-Y. Cho, G. Cao, J. Yu, S. J. Moon, and T. W. Noh, *Phys. Rev. B* **88**, 085125 (2013).
- <sup>7</sup> H.-J. Kim, J.-H. Lee, and J.-H. Cho, *Sci. Rep.* **4**, 5253 (2014).
- <sup>8</sup> M. Kim, B. H. Kim, and B. I. Min, *Phys. Rev. B* **93**, 195135 (2016).
- <sup>9</sup> I. I. Mazin, H. O. Jeschke, K. Foyevtsova, R. Valentí, and D. I. Khomskii, *Phys. Rev. Lett.* **109**, 197201 (2012).
- <sup>10</sup> Y. Yamaji, Y. Nomura, M. Kurita, R. Arita, and M. Imada, *Phys. Rev. Lett.* **113**, 107201, (2014).
- <sup>11</sup> K. Foyevtsova, H. O. Jeschke, I. I. Mazin, D. I. Khomskii, and R. Valentí, *Phys. Rev. B* **88**, 035107 (2013).
- <sup>12</sup> J. Chaloupka, G. Jackeli, and G. Khaliullin, *Phys. Rev. Lett.* **105**, 027204 (2010).
- <sup>13</sup> Y. Singh, S. Manni, J. Reuther, T. Berlijn, R. Thomale, W. Ku, S. Trebst, and P. Gegenwart, *Phys. Rev. Lett.* **108**, 127203 (2012).
- <sup>14</sup> K. W. Plumb, J. P. Clancy, L. J. Sandilands, V. V. Shankar, Y. F. Hu, K. S. Burch, H.-Y. Kee, and Y.-J. Kim, *Phys. Rev. B* **90**, 041112(R) (2014).
- <sup>15</sup> L. J. Sandilands, Y. Tian, K. W. Plumb, Y.-J. Kim, and K. S. Burch, *Phys. Rev. Lett.* **114**, 147201 (2015).
- <sup>16</sup> H.-S. Kim, V. V. Shankar, A. Catuneanu, and H.-Y. Kee, *Phys. Rev. B* **91**, 241110(R) (2015).
- <sup>17</sup> J. Chaloupka, and G. Khaliullin, *Phys. Rev. B* **94**, 064435 (2016).

- <sup>18</sup> F. Ye, S. Chi, H. Cao, B. C. Chakoumakos, J. A. F-Baca, R. Custelcean, T. F. Qi, O. B. Korneta, and G. Cao, Phys. Rev. B **85** 180403(R)(2012).
- <sup>19</sup> X. Liu, T. Berlijn, W.-G. Yin, W. Ku, A. Tsvelik, Y.-J. Kim, H. Gretarsson, Y. Singh, P. Gegenwart, and J. P. Hill, Phys. Rev. B **83** 220403 (2011).
- <sup>20</sup> I. Kimchi and Y.-Z. You, Phys. Rev. B **84** 180407(R) (2011).
- <sup>21</sup> L. Sizyuk, C. Price, P. Wölfle, and N. B. Perkins, Phys. Rev. B **90** 155126 (2014).
- <sup>22</sup> J. G. Rau, E. Kin-Ho Lee, and H.-Y. Kee, Phys. Rev. Lett. **112** 077204 (2014).
- <sup>23</sup> L. Janssen, E. C. Andrade, and M. Vojta, arXiv:1706.05380 (2017).
- <sup>24</sup> R. D. Johnson, S. C. Williams, A. A. Haghighirad, J. Singleton, V. Zapf, P. Manuel, I. I. Mazin, Y. Li, H. O. Jeschke, R. Valent, and R. Coldea, Phys. Rev. B **92**, 235119 (2015).
- <sup>25</sup> M. Majumder, M. Schmidt, H. Rosner, A. A. Tsirlin, H. Yasuoka, and M. Baenitz, Phys. Rev. B **91**, 180401(R) (2015).
- <sup>26</sup> Y. Kubota, H. Tanaka, T. Ono, Y. Narumi, and K. Kindo, Phys. Rev. B **91**, 094422 (2015).
- <sup>27</sup> J.-I. Igarashi and T. Nagao, J. Electron Spectrosc. Relat. Phenom. **212** 44 (2016).
- <sup>28</sup> L. Liang, Z. Wang, and Y. Yu, Phys. Rev. B **90**, 075119 (2014).
- <sup>29</sup> G. Jackeli, G. Khaliullin Phys. Rev. Lett. **102**, 017205 (2009).
- <sup>30</sup> S. Mohapatra, J. van den Brink, and A. Singh, Phys. Rev. B **95**, 094435 (2017).
- <sup>31</sup> A. Singh, Phys. Rev. B **71**, 214406 (2005).
- <sup>32</sup> S. M. Winter, A. A. Tsirlin, M. Daghofer, J. van den Brink, Y. Singh, P. Gegenwart and R. Valentí, J. Phys.: Condens. Matter **29**, 493002 (2017).